Journal of Experimental Botany, Vol. 66, No. 13 pp. 3959–3975, 2015
doi:10.1093/jxb/erv196 Advance Access publication 8 May 2015
This paper is available online free of all access charges (see http://jxb.oxfordjournals.org/open_access.html for further details)

RESEARCH PAPER

The floral transcriptome of ylang ylang (*Cananga odorata* var. *fruticosa*) uncovers biosynthetic pathways for volatile organic compounds and a multifunctional and novel sesquiterpene synthase

Jingjing Jin[1,2,*], Mi Jung Kim[1,*], Savitha Dhandapani[1,3], Jessica Gambino Tjhang[1], Jun-Lin Yin[1], Limsoon Wong[2], Rajani Sarojam[1], Nam-Hai Chua[4], and In-Cheol Jang[1,3,†]

[1] Temasek Life Sciences Laboratory, 1 Research Link, National University of Singapore, Singapore 117604
[2] School of Computing, National University of Singapore, Singapore 117417
[3] Department of Biological Sciences, National University of Singapore, Singapore 117543
[4] Laboratory of Plant Molecular Biology, The Rockefeller University, 1230 York Avenue, New York, NY 10065, USA

* These authors contributed equally to this study.
† To whom correspondence should be addressed. E-mail: jangi@tll.org.sg

Received 17 February 2015; Revised 23 March 2015; Accepted 25 March 2015

Abstract

The pleasant fragrance of ylang ylang varieties (*Cananga odorata*) is mainly due to volatile organic compounds (VOCs) produced by the flowers. Floral scents are a key factor in plant–insect interactions and are vital for successful pollination. *C. odorata* var. *fruticosa*, or dwarf ylang ylang, is a variety of ylang ylang that is popularly grown in Southeast Asia as a small shrub with aromatic flowers. Here, we describe the combined use of bioinformatics and chemical analysis to discover genes for the VOC biosynthesis pathways and related genes. The scented flowers of *C. odorata* var. *fruticosa* were analysed by gas chromatography/mass spectrometry and a total of 49 VOCs were identified at four different stages of flower development. The bulk of these VOCs were terpenes, mainly sesquiterpenes. To identify the various terpene synthases (TPSs) involved in the production of these essential oils, we performed RNA sequencing on mature flowers. From the RNA sequencing data, four full-length TPSs were functionally characterized. *In vitro* assays showed that two of these TPSs were mono-TPSs. CoTPS1 synthesized four products corresponding to β-thujene, sabinene, β-pinene, and α-terpinene from geranyl pyrophosphate and CoTPS4 produced geraniol from geranyl pyrophosphate. The other two TPSs were identified as sesqui-TPSs. CoTPS3 catalysed the conversion of farnesyl pyrophosphate to α-bergamotene, whereas CoTPS2 was found to be a multifunctional and novel TPS that could catalyse the synthesis of three sesquiterpenes, β-ylangene, β-copaene, and β-cubebene. Additionally, the activities of the two sesqui-TPSs were confirmed *in planta* by transient expression of these TPS genes in *Nicotiana benthamiana* leaves by *Agrobacterium*-mediated infiltration.

Key words: β-Copaene, β-cubebene, β-ylangene, *Cananga odorata* var. *fruticosa*, floral scent, terpene synthase, terpenes, volatile organic compounds, ylang ylang.

Abbreviations: CaMV, cauliflower mosaic virus; FPP, farnesyl pyrophosphate; GC-MS, gas chromatography/mass spectrometry; GO, Gene Ontology; GPP, geranyl pyrophosphate; HMGR, 3-hydroxy-3-methylglutaryl-CoA reductase; MEP, 2-C-methyl-d-erythritol 4-phosphate; MVA, mevalonate; ORF, open reading frame; qRT-PCR, quantitative real-time reverse transcription PCR; RI, retention index; RNA-seq, RNA sequencing; Tp, transit peptide; TPS, terpene synthase; VOC, volatile organic compound; YFP, yellow fluorescent protein.

Introduction

Plants emit a large group of phytogenic volatile organic compounds (VOCs) for their defence against pathogens, parasites, and herbivores, and for attracting pollinators (Kessler and Baldwin, 2001; Dudareva *et al.*, 2013). VOCs are synthesized in all plant organs such as flowers, stems, leaves, roots, fruits and seeds, but the quantity and diversity of VOCs change in response to environmental stimuli (Dudareva *et al.*, 2013). VOCs are major components of floral scent in a wide range of flowers (Knudsen *et al.*, 1993). Over 1700 floral VOCs have been identified from 90 different plants, and they are assumed to function in both attraction of pollinators and defence against pathogens (Knudsen *et al.*, 2006; Muhlemann *et al.*, 2014). Given the important role of VOCs, their production and emission are highly regulated both spatially and developmentally.

Floral VOCs are mainly composed of terpenoids, phenylpropanoids/benzenoids, and volatile fatty acid derivatives, which are derived from different biosynthetic routes in plants (Muhlemann *et al.*, 2014). Terpenoids, also referred to as isoprenoids, are the largest and most diverse class of VOCs in plants (Dudareva *et al.*, 2013). Terpenes are synthesized from two distinct and compartmentally separated pathways, the mevalonate (MVA) and 2-C-methyl-D-erythritol 4-phosphate (MEP) pathways (McGarvey and Croteau, 1995). The phenylpropanoid and benzenoid class of metabolites is derived primarily from the carbon skeleton of phenylalanine, which is produced by the shikimate pathway (Orlova *et al.*, 2006; Vogt, 2010).

Terpene synthases (TPSs) are responsible for generating the immense diversity in terpenes produced by plants (McGarvey and Croteau, 1995). Many TPSs have the ability to synthesize multiple products from a single prenyl diphosphate substrate (Degenhardt *et al.*, 2009). Based on sequence relatedness and functional assessment, the TPS gene family has been divided into seven subfamilies designated TPS-a to TPS-g (Bohlmann *et al.*, 1998; Lee and Chappell, 2008; Martin *et al.*, 2010). The TPS-a subfamily typically contains angiosperm-specific sesqui-TPSs, whereas angiosperm mono-TPSs form the TPS-b subfamily. The TPS-b subfamily contains the arginine/tryptophan motif R(R)X_8W, which plays a role in the RR-dependent isomerization of GPP (Martin *et al.*, 2010). Another angiosperm mono-TPS subfamily, TPS-g, contains mono-TPSs that lack the R(R)X_8W motif. These TPSs produce acyclic monoterpenes that contribute to the floral VOCs (Dudareva *et al.*, 2013). The TPS-c and TPS-e subfamilies consist of angiosperm di-TPSs responsible for gibberellic acid biosynthesis, namely copalyl diphosphate synthases and kaurene synthases. The different mono-, sesqui-, and di-TPS genes encoding enzymes for the synthesis of conifer-specialized terpenes belong to the gymnosperm-specific TPS-d subfamily (Martin *et al.*, 2004). TPS-f includes the monoterpene linalool synthase of the genus *Clarkia* (Dudareva *et al.*, 1996).

Cananga odorata, commonly called ylang ylang, is a tropical evergreen tree of the family *Annonaceae* that produces fragrant flowers and is widely cultivated throughout Southeast Asia. Essential oils obtained by steam distillation from mature fresh ylang ylang flowers are used in the cosmetic industry as major components of perfumes and fragrances, in the food industry as ingredients of aromas and flavours, and in the pharmaceutical industry as active components of antibacterials and in aromatherapy (Gaydou *et al.*, 1986; Burdock and Carabin, 2008; Benini *et al.*, 2010). The chemical composition of floral VOCs produced by ylang ylang varieties has been reported previously (Gaydou *et al.*, 1986; Benini *et al.*, 2010, 2012; Brokl *et al.*, 2013). These studies showed the presence of the volatile terpenes benzenoid and phenylpropanoid in floral VOCs. Gaydou *et al.* (1986) described the composition of essential oils of ylang ylang flowers originating from Madagascar (*C. odorata* Hook Fil. et Thomson forma genuina). These authors found that the primary component was the monoterpene linalool (19%), and the other major compounds were two sesquiterpenes, β-caryophyllene (10.7%) and germacrene D (10.3%). Additionally, this variety of ylang ylang from Madagascar contained more than 20% of other aromatic compounds such as *p*-methylanisole, benzyl benzoate, methyl benzoate, and benzyl salicylate (Gaydou *et al.*, 1986). *C. odorata* var. *fruticosa*, or dwarf ylang ylang, is another variety that is popularly grown in Southeast Asia as a small, compact shrub with highly scented flowers. Its essential oil is also used in the perfume industry. Despite the economic and social importance of this species, biosynthetic pathways leading to the production of the floral scent of this ylang ylang variety are not yet fully understood.

High-throughput RNA sequencing (RNA-seq) has increasingly become the method of choice to discover genes for metabolic pathways. We determined the chemical composition of floral VOCs at four different stages of flower formation and performed RNA-seq on mature yellow flowers of *C. odorata* var. *fruticosa* where the production of floral VOCs is at the maximum. Terpenes formed the bulk of floral VOCs in this variety. Our transcriptome data revealed 16 TPS transcripts from dwarf ylang ylang flowers of which four were functionally characterized in this study.

Materials and methods

Plant materials

The yellow flowers of *C. odorata* var. *fruticosa* (dwarf ylang ylang) grown in Singapore were collected in November for RNA-seq. Four different stages of flowers and leaves of dwarf ylang ylang were obtained in April for further experiments. The four different stages of flowers were as follows: B, bud stage: completely closed petal, green; I, initial-flowering stage: semi-open small and short petals, green, 9 d after bud stage; II, full-flowering stage: completely open large and long petals, yellowish green, 20 d after bud stage; and III, end-flowering stage: fully matured petals, yellow, 30 d after bud stage.

Four-week-old *Nicotiana benthamiana* plants grown in a greenhouse were used for *in vivo* characterization and subcellular localization of CoTPSs.

Extraction of essential oils from ylang ylang flowers

Flowers and leaves from ylang ylang were frozen in liquid nitrogen and ground to a powder with a pre-chilled mortar and pestle. About

500 mg of powder was dissolved in 500 µl of ethyl acetate (Fisher Scientific) including 1 µl (10 mg ml^{-1}) of camphor (Sigma-Aldrich) as an internal standard. The slush was vortexed and incubated on a horizontal shaker at 50 rpm for 2 h. After centrifugation of the mixture at 13 000*g* for 10 min, the resulting ethyl acetate upper layer extract was transferred to a clean Eppendorf tube and mixed with 300 mg of anhydrous Na_2SO_4 (Sigma-Aldrich) to remove water. Following the second centrifugation, the extract was transferred into a 2 ml glass vial for gas chromatography/mass spectrometry (GC-MS) analysis (Agilent Technologies).

RNA isolation for RNA sequencing

Frozen ylang ylang flowers were homogenized using a pre-chilled mortar and pestle into a fine powder, and total RNA was isolated using the TRIzol method (Invitrogen). Purified RNA samples were first treated with RNase-free DNase I (Roche) to remove genomic DNA and then extracted using chloroform. The RNA quantity was determined with a Nanodrop spectrophotometer (ND-1000; Thermo Fisher Scientific). The RNA integrity number (RIN) was evaluated using an Agilent 2100 bioanalyzer and RNA 6000 Nano Labchip kit (Agilent Technologies). RNA with a RIN value of $7<x<10$ was sent for RNA-seq to the Rockefeller University Genomics Resource Center (New York, USA). RNA-seq and assembly were carried out as described by Jin *et al.* (2014).

Quantitative real-time reverse transcription PCR (qRT-PCR)

Quantitative RT-PCR was performed to investigate gene expression patterns during ylang ylang flower development. One microgram of total RNA was used for first-strand cDNA synthesis with Moloney murine leukemia virus reverse transcriptase (Promega). The qRT-PCRs were performed using an Applied Biosystems 7900HT Fast Real-time PCR System and Applied Biosystems Power SYBR Green PCR Master Mix (Life Technologies). Oligonucleotide primers for qRT-PCR were designed for selected genes of the MEP, MVA, shikimate, benzyl, and phenyl propanoid pathways using Primer3 (http://bioinfo.ut.ee/primer3-0.4.0/) and are listed in Supplementary Table S1, available at *JXB* online. Each PCR product obtained from regular PCR was cloned into the pGEM-T Easy vector (Promega) and verified by sequencing. The specificity of the amplified PCR product was assessed by melting-curve analysis. All experiments were carried out in technical triplicates and with biological duplicates. A non-template control was included for each gene to exclude random/reagent contamination and primer-dimer formation. A mock reaction containing all the RT-PCR reagents except the reverse transcriptase was used as a negative control. The *Actin* gene was used for normalization in each qRT-PCR.

Sequence identification, multiple sequence alignment and phylogenetic analysis

DNA sequences were edited and assembled using Lasergene 8 (DNASTAR). The phylogenetic analysis of CoTPSs was performed using the maximum likelihood method in MEGA version 6 (Tamura *et al.*, 2011).

Isolation of the full-length open reading frame (ORF) of CoTPS and vector construction for Agrobacterium*-mediated gene expression*

Full-length ORFs of *CoTPS* genes were amplified by PCR from dwarf ylang ylang flower-derived cDNA with the primer sets listed in Supplementary Table S1. Purified PCR products were cloned into pENTR/D-TOPO (Invitrogen). For yellow fluorescent protein (YFP) fusion constructs, the pTOPO clone harbouring each *CoTPS* gene was integrated into the destination vector, the pBA-DC-YFP expression vector (Zhang *et al.*, 2005), which contains the cauliflower mosaic virus (CaMV) 35S promoter and the C-terminal in-frame *YFP* gene to create *CoTPS–YFP* using LR Clonase (Invitrogen). All constructs were verified by DNA sequencing. The final plasmid was transformed into *Agrobacterium tumefaciens* GV3101 by electroporation (Bio-Rad), plated on an LB plate containing spectinomycin (100 µg ml^{-1}) and gentamycin (20 µg ml^{-1}), and incubated at 28 °C for 2 d.

Subcellular localization of CoTPSs

Agrobacterium-mediated transient gene expression was performed using leaves of 4-week-old *N. benthamiana* plant as described by Jin *et al.* (2014). Infiltrated *N. benthamiana* leaves expressing YFP-fused protein were excised, mounted on slides, and imaged using a confocal laser-scanning microscope (Carl Zeiss LSM5 Exciter) with a standard filter set. Images were processed with the LSM Image Browser (Carl Zeiss).

Preparation of recombinant proteins

To construct vectors for the recombinant N-terminal poly-histidine (6His)-tagged proteins, the full-length ORF of *CoTPS* was amplified by PCR with primers designed with restriction enzymes sites at the ends (Supplementary Table S1). The PCR-amplified product and pET28b plasmid (Novagen) were digested separately with the corresponding restriction enzymes (New England Biolabs) and purified using a Qiagen PCR Purification kit. The digested PCR product was then cloned into the pET28b expression vector using a Rapid DNA Ligation kit (Roche). The final construct was transformed into *Escherichia coli* BL21(DE3)pLysS (Invitrogen), and recombinant proteins were purified from *E.coli* extracts after isopropyl β-D-1-thiogalactopyranoside induction as described previously (Jang *et al.*, 2005).

In vitro *TPS assay*

An *in vitro* enzyme assay for TPS activity was performed in a final volume of 500 µl of reaction buffer [25 mM HEPES, pH 7.4, 100 mM KCl, 7.5 mM $MgCl_2$, 5% (v/v) glycerol, 5 mM dithiothreitol], with about 20 µg of recombinant protein and 10 µg of either farnesyl pyrophosphate (FPP) or geranyl pyrophosphate (GPP) (Sigma-Aldrich). The reaction mixtures were mixed gently and carefully overlaid with 250 µl of hexane (Sigma-Aldrich) to trap volatile products. The tube was then sealed with Parafilm and incubated at 30 °C for 2 h, followed by 1 min of vortexing. After centrifugation at 1200*g* at 4 °C for 30 min, the hexane upper layer was transferred into a 2 ml glass vial for GC-MS analysis (see below). As a negative control, heat-inactivated recombinant protein was added to the enzyme assay.

In vivo *characterization of CoTPSs*

The underside of *N. benthamiana* leaves was infiltrated with an *Agrobacterium* strain harbouring the *CoTPS* construct with or without the strain carrying *Arabidopsis* 3-hydroxy-3-methylglutaryl-CoA reductase (*AtHMGR*) under the control of a CaMV 35S promoter (Jin *et al.*, 2014). All experiments were carried out with co-expression of the viral-encoded protein P19, which improves transgene expression by suppressing post-transcriptional gene silencing (Voinnet *et al.*, 2003). After infiltration, the tobacco plants were maintained in a growth chamber at 25 °C, under long-day conditions (16 h light/8 h dark) for 3 d. Four to five infiltrated leaves were then frozen immediately in liquid nitrogen and homogenized with a pre-chilled mortar and pestle. Up to 400–600 mg of leaf powder was obtained from four to five leaves. Subsequent sample processing for GC-MS analysis was performed as described above. A *CaMV35S::AtHMGR* construct served as a negative control.

GC-MS analysis

GC-MS analysis was performed on an Agilent 7890A GC system and an Agilent Technologies 5975C Inert XL Mass Selective Detector, equipped with an HP-5MS UI column (30 m×0.25 mm×0.25 µm; Agilent Technologies). Conditions were as follows: 5 µl sample injection, splitless injection, oven program 50 °C (1 min hold) at 8 °C min^{-1} to 300 °C (5 min hold). For data processing, MSD ChemStation Data Analysis (Agilent Technologies) was used. The essential oil components were identified by comparison of their mass spectra with those in the NIST 2011 library data for GC-MS and comparison of their retention indices (RIs). The RIs were determined on the basis of an *n*-alkanes (C8–C40) mix standard (Sigma-Aldrich) under the same operation conditions. Camphor was added to serve as an internal standard. The amount of each compound was calculated by measuring its peak area related to that of a known amount of camphor. The identified components along with their RIs and relative percentage values are listed in Table 1.

Accession number

The RNA-seq data supporting this study are available in the DNA Data Bank of Japan (DDBJ: http://www.ddbj.nig.ac.jp/) under accession number DRA002822.

Results

Stage-specific variations of VOCs in dwarf ylang ylang flowers

Flowers can emit different volatile compounds at different stages of development (Dudareva *et al.*, 2000). Dwarf ylang ylang flowers have little floral scent when the petals are green, but their scent gradually becomes stronger as the flower matures. To examine the overall intensity and the diversity of the floral scent during flower development, total essential oils from flowers at four different stages of development were analysed by GC-MS (Fig. 1). Figure 1B and Supplementary Fig. S1 show that the chemical composition of the essential oils from the floral bud stage to the three different stages of open flower development was very diverse, both quantitatively and qualitatively. Only 15 compounds that had meaningful levels of >0.1% of total volatile compounds were detected from floral buds (Fig. 1B, Table 1). The number of peaks increased progressively during maturation of flower buds into fully open flowers. More than 20, 27, and 45 volatile compounds were obtained from the three different stages of flower development: undeveloped small flower (I), mature green flower (II), and fully mature yellow flower (III). Hence, the fully mature stage represents the stage where there was maximum production of VOCs by the flowers. At this stage, the majority of the volatiles were terpenes with a few benzenoid/phenolpropanoid compounds. Out of 45 compounds identified, 31 were identified as mono- and sesquiterpenes using the mass spectra reference library (Fig. 1B and Table 1). Interestingly, >90% of the total identified terpenes were sesquiterpenes consisting of α-farnesene (31.50%), α-bergamotene (26.79%), germacrene D (13.26%), β-caryophyllene (11.57%), humulene (1.63%), farnesol (0.75%), *trans*-β-farnesene (0.77%), and β-ylangen (0.63%), whereas monoterpenes were quantitatively less than 10%, comprising mainly *cis*-β-ocimene (1.99%), *trans*-β-ocimene (1.55%), and β-linalool (1.40%). Other aromatic compounds comprised <3%. The relative amounts of all identified volatiles are shown in Table 1 (see mature yellow flowers, III). Dried yellow flowers of ylang ylang also showed a similar volatile composition (Supplementary Fig. S2A, available at *JXB* online). Compared with flowers, ylang ylang leaves contained very low levels of terpenes, comprising mainly α-pinene, β-caryophyllene, germacrene D, and phytol (Supplementary Fig. S2B).

Two sesquiterpenes, germacrene D and β-caryophyllene, could be found at all stages of development, and their levels were retained or slightly decreased during open flower development (#22 and #28, Fig. 1B, and Supplementary Fig. S3, available at *JXB* online). However, the other two major sesquiterpenes, α-farnesene and α-bergamotene, were undetectable at the floral bud stage but were found during early flower development (#29 and #30 in I, Fig. 1B, and Supplementary Fig. S3) and subsequently became the most abundant components of essential oils at mature stages of flower development (II and III, Fig. 1B). Interestingly, most of the monoterpenes except α-pinene were undetectable at the floral bud stage, but they gradually increased during open flower development (Fig. 1B). Among the monoterpenes, *trans*-β-ocimene, β-ocimene, and β-linalool were highly inducible during flower maturation (#9, #10, and #13, Fig. 1B). Additionally, our GC-MS analysis identified several sesquiterpenes or sesquiterpene alcohols that decreased during flower maturation such as δ-elemene (#46), α-ylangene (#47), γ-cadinene (#48), and α-copaene-11-ol (#49). Other aromatic compounds such as benzenoid/phenolpropanoid and volatile fatty acids were found almost exclusively in mature yellow flowers (Fig. 1B and Supplementary Fig. S1, Table 1). GC-MS analysis of flowers at night did not show any change in VOC profile, suggesting that there are no significant diurnal changes in the emission pattern (Supplementary Fig. S4, available at *JXB* online).

RNA sequencing, de novo *assembly, and annotation of the transcriptome*

To profile the dwarf ylang ylang floral transcriptome, we sequenced RNA-seq libraries synthesized from the mature yellow flowers. Illumina sequencing runs generated more than 110 million reads of 101 bp, and the quality of reads was evaluated by FastQC (http://www.bioinformatics.babraham.ac.uk/projects/fastqc/) (Supplementary Fig. S5, available at *JXB* online). Due to the absence of reference genomic sequences for ylang ylang, the Trinity method was used for *de novo* assembly of short sequence reads (Grabherr *et al.*, 2011). These assemblies generated a total of 45 379 unigenes with an N50 value of 2016 bp (Table 2). The assembled unigenes were BLASTed against the National Centre for Biotechnology Information non-redundant (nr) protein database and protein databases for *Arabidopsis thaliana*, *Vitis vinifera*, and *Oryza sativa*. Among 45 379 unigenes, 30 539 unigenes (67.3%) were annotated through a BlastX search with E-values ≤1e–3 (Table 2). Functional classifications of Gene Ontology (GO) terms of all unigenes were performed using Trinotate (Quevillon *et al.*, 2005). Figure 2

Table 1. *Essential oils composition of the flowers from* C. odorata var. fruticosa

No.[a]	Compounds	RT (min)[b]	RI[c]	Formula	RA (%)[d]			
					Bud	I	II	III
1	β-Thujene	9.507	904	$C_{10}H_{16}$	–	–	0.21	0.36
2	α-Pinene	9.652	919	$C_{10}H_{16}$	3.08	1.30	0.99	0.65
3	Camphene	9.894	943	$C_{10}H_{16}$	–	–	–	0.13
4	Sabinene	10.199	974	$C_{10}H_{16}$	–	–	0.26	0.43
5	β-Pinene	10.342	988	$C_{10}H_{16}$	–	–	0.45	0.66
6	α-Phellandrene	10.661	993	$C_{10}H_{16}$	–	–	–	0.05
7	α-Terpinene	10.846	1012	$C_{10}H_{16}$	–	–	–	0.27
8	p-Cresol methyl ether	10.884	1016	$C_8H_{10}O$	–	–	–	0.49
9	*trans*-β-Ocimene	11.054	1023	$C_{10}H_{16}$	–	0.46	0.88	1.55
10	β-Ocimene	11.170	1024	$C_{10}H_{16}$	–	0.40	1.09	1.99
11	γ-Terpinene	11.397	1027	$C_{10}H_{16}$	–	–	–	0.15
12	Terpinolene	12.011	1032	$C_{10}H_{16}$	–	–	–	0.16
13	β-Linalool	12.102	1040	$C_{10}H_{18}O$	–	0.38	0.99	1.40
14	Neo-allo-ocimene	12.594	1089	$C_{10}H_{16}$	–	–	–	0.18
15	3,4-Dimethoxytoluene	14.460	1197	$C_9H_{12}O_2$	–	–	–	0.39
16	2-Methoxy-4-vinylphenol	15.854	1276	$C_9H_{10}O_2$	–	–	–	0.19
17	γ-Elemene	16.176	1306	$C_{15}H_{24}$	–	–	–	0.16
18	Eugenol	16.481	1309	$C_{10}H_{12}O_2$	–	–	–	0.17
19	α-Copaene	16.831	1321	$C_{15}H_{24}$	1.81	1.24	0.83	0.44
20	γ-Gurjunene	17.025	1340	$C_{15}H_{24}$	3.00	1.16	0.56	0.32
21	Methyleugenol	17.062	1344	$C_{11}H_{14}O_2$	–	–	–	0.08
22	β-Caryophyllene	17.600	1398	$C_{15}H_{24}$	16.47	23.50	15.90	11.57
23	β-Ylangene	17.683	1406	$C_{15}H_{24}$	3.55	1.80	1.16	0.63
24	(E)-β-Farnesene	17.836	1421	$C_{15}H_{24}$	–	0.51	0.61	0.77
25	γ-Muurolene	17.910	1429	$C_{15}H_{24}$	1.21	0.60	0.38	0.20
26	Humulene	18.020	1440	$C_{15}H_{24}$	3.44	3.44	2.24	1.63
27	β-Cubebene	18.110	1449	$C_{15}H_{24}$	1.02	0.35	0.19	0.08
28	GermacreneD	18.580	1450	$C_{15}H_{24}$	50.17	33.17	27.33	13.26
29	α-Farnesene	18.686	1461	$C_{15}H_{24}$	–	10.03	19.89	31.50
30	α-Bergamotene	18.771	1469	$C_{15}H_{24}$	–	18.67	23.63	26.79
31	Cedrene	18.932	1485	$C_{15}H_{24}$	–	–	0.32	0.33
32	δ-Cadinene	18.989	1491	$C_{15}H_{24}$	1.54	0.43	0.17	0.17
33	α-Patchoulene	19.035	1495	$C_{15}H_{24}$	–	–	0.07	0.13
34	Elemicin	19.233	1515	$C_{12}H_{16}O_3$	–	–	–	0.13
35	Germacrene D-4-ol	19.845	1537	$C_{15}H_{26}O$	0.75	0.21	0.16	0.13
36	β-Caryophyllene oxide	19.950	1548	$C_{15}H_{24}O$	–	–	–	0.07
37	Isoelemicin	20.561	1609	$C_{12}H_{16}O_3$	–	–	0.15	0.13
38	Farnesol	21.527	1763	$C_{15}H_{26}O$	–	0.88	0.85	0.75
39	Benzyl benzoate	22.236	1812	$C_{14}H_{12}O_2$	–	–	0.27	0.69
40	*cis*-11-Hexadecenal	22.505	1830	$C_{16}H_{30}O$	–	–	–	0.11
41	Octadecanal	22.623	1841	$C_{18}H_{36}O$	–	–	–	0.07
42	(E,E,) farnesol acetate	22.941	1873	$C_{17}H_{28}O_2$	–	–	0.10	0.10
43	Z-9-Hexadecen-1-ol	23.328	1912	$C_{16}H_{32}O$	–	–	–	0.17
44	9-Nonadecene	23.475	1918	$C_{19}H_{38}$	–	–	–	0.18
45	Benzyl salicylate	23.600	1931	$C_{14}H_{12}O_3$	–	–	–	0.21
46	δ-Elemene	16.173	1308	$C_{15}H_{24}$	4.81	0.98	0.34	–
47	α-Ylangene	18.662	1458	$C_{15}H_{24}$	7.16	–	–	–
48	γ-Cadinene	18.910	1483	$C_{15}H_{24}$	1.31	0.52	–	–
49	α-Copaene-11-ol	21.094	1720	$C_{15}H_{24}O$	0.67	–	–	–

[a] Compounds listed in order of elution from a HP-5MS UI column.
[b] RT, retention time (min).
[c] RI, retention indices calculated against C_8–C_{40} *n*-alkanes on the HP-5MS UI column.
[d] RA, relative amount (%); ratio expressed against the sum of all peaks.

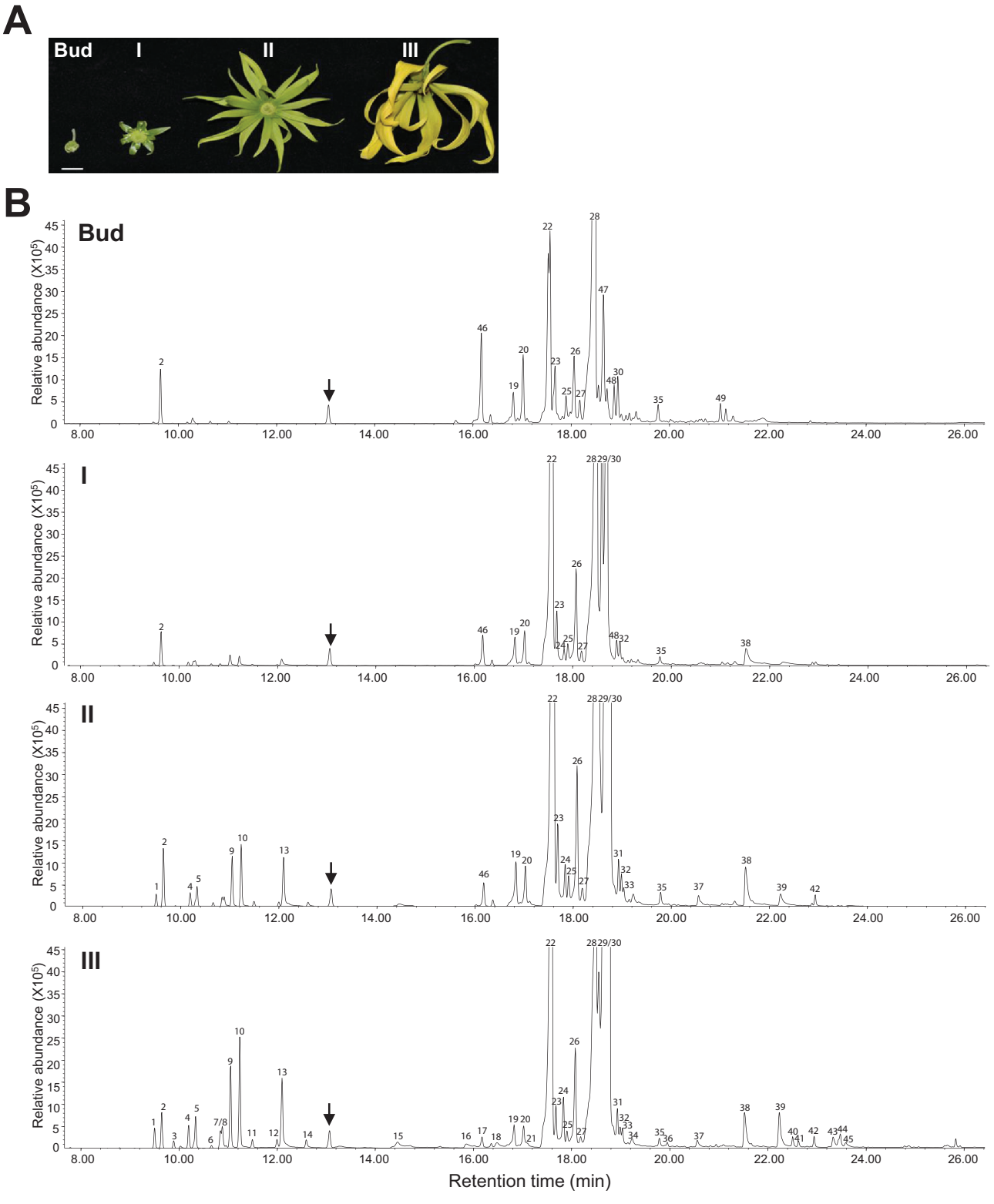

Fig. 1. Compositional variation of dwarf ylang ylang essential oils during flower development. (A) Photograph of dwarf ylang ylang flowers showing the development of a newly emerged flower bud to a fully open yellow flower. I, Undeveloped small flower; II, mature green flower; III, fully mature yellow flower. Bar, 1 cm. (B) GC traces of essential oils from floral buds, undeveloped small flowers (I), mature green flowers (II), and fully mature yellow flowers (III). The arrows indicate the peak of camphor (10 μg μl^{-1}), the internal standard used in the assay. The peaks numbered in the traces are identical to those listed in Table 1. The traces are magnified images of the corresponding zones indicated by a dotted line in Supplementary Fig. S1, available at *JXB* online. (This figure is available in colour at *JXB* online.)

shows enriched GO terms for the top 1000 highly expressed transcripts. From our annotated unigenes, 16 were identified as TPSs that were more than 500 bp. Of these, four unigenes contained full-length ORFs encoding TPS.

RNA-seq analysis of different biosynthetic pathways active in flowers

GC-MS analysis of the mature flowers showed that the majority of VOCs were terpenes. We used our RNA-seq data

to analyse the expression profile of genes encoding enzymes for the precursor pathways leading to the formation of VOCs in mature flowers. The majority of ylang ylang orthologue unigenes were full length and showed high sequence similarity to known enzymes of these pathways from other plants (Supplementary Fig. S6, available at *JXB* online).

The MEP and MVA pathways are the pathways leading to the formation of mono- and sesquiterpenes. Transcripts of all the enzyme genes involved in these two pathways were detected in our RNA-seq data, and their expression was validated by qRT-PCR (Fig. 3). Additionally, the expression of these enzyme genes was also examined at earlier stages of flower development and in leaves by qRT-PCR. Genes encoding the MEP and MVA enzymes were active in all stages of flower development consistent with the high production of terpenes in the flowers (Fig. 3A, B). It has been reported that 1-deoxy-D-xylulose-5-phosphate synthase (DXS), the first enzyme of the MEP pathway, is important for the overall regulation of the pathway and is encoded by a small gene family (Cordoba *et al.*, 2011). From our RNA-seq data, we were able to identify four different *DXS* unigenes showing different levels of abundance in flowers and leaf. One of these, *DXS3*, belonging to clade 2, which may be related to secondary metabolism (Walter *et al.*, 2002; Phillips *et al.*, 2007), was highly induced in stage III flowers (Fig. 3A and Supplementary Figs S7 and Fig. S8, available at *JXB* online). The majority of the genes, except phenylalanine ammonia lyase (*PAL*), for the shikimate pathway enzymes, which produce phenylalanine for the production of benzonoids and phenylproponids, appeared to be expressed more in mature flowers (Fig. 3C, D). The significant benzenoids in VOCs were benzyl benzoate and benzyl salicylate, and the phenylproponoid was eugenol. These compounds were detected only in mature flowers (#18, #39, and #45, Fig. 1B, Table 1). Previous *in vitro* experiments have indicated that benzyl benzoate might play a role in pollinator attraction (Hoballah *et al.*, 2005; Huber *et al.*, 2005) or in plant defence (miticide) (Harju *et al.*, 2004).

Table 2. *Overview of the assembly results of RNA-seq*

No. isoforms	N50 (bp)	No. unigenes	No. annotated	% Annotation
86 512	2016	45 379	30 539	67.3

Phylogenetic analysis of TPS *genes from dwarf ylang ylang flowers*

Terpenes were the major VOCs of dwarf ylang ylang flowers. From the dwarf ylang ylang RNA-seq data, four full-length ORFs of *TPS* genes were PCR amplified from cDNA pools of the flowers. Phylogenetic analysis based on the deduced amino acid sequences of four *CoTPS* cDNAs showed that CoTPS2 (561 aa) belonged to the TPS-a subfamily representing the sesqui-TPSs, whereas CoTPS1 (590 aa) and CoTPS3 (547 aa) fell into the TPS-b subfamily, which consists mainly of mono-TPSs (Chen *et al.*, 2011; Fig. 4A). CoTPS4 (586 aa) is a member of the TPS-g subfamily, which lacks the R(R)X_8W motif in the N-terminal region of mono-TPSs and produces acyclic monoterpenes (Dudareva *et al.*, 2003; Yuan *et al.*, 2008; Chen *et al.*, 2011; Fig. 4A). All four CoTPSs

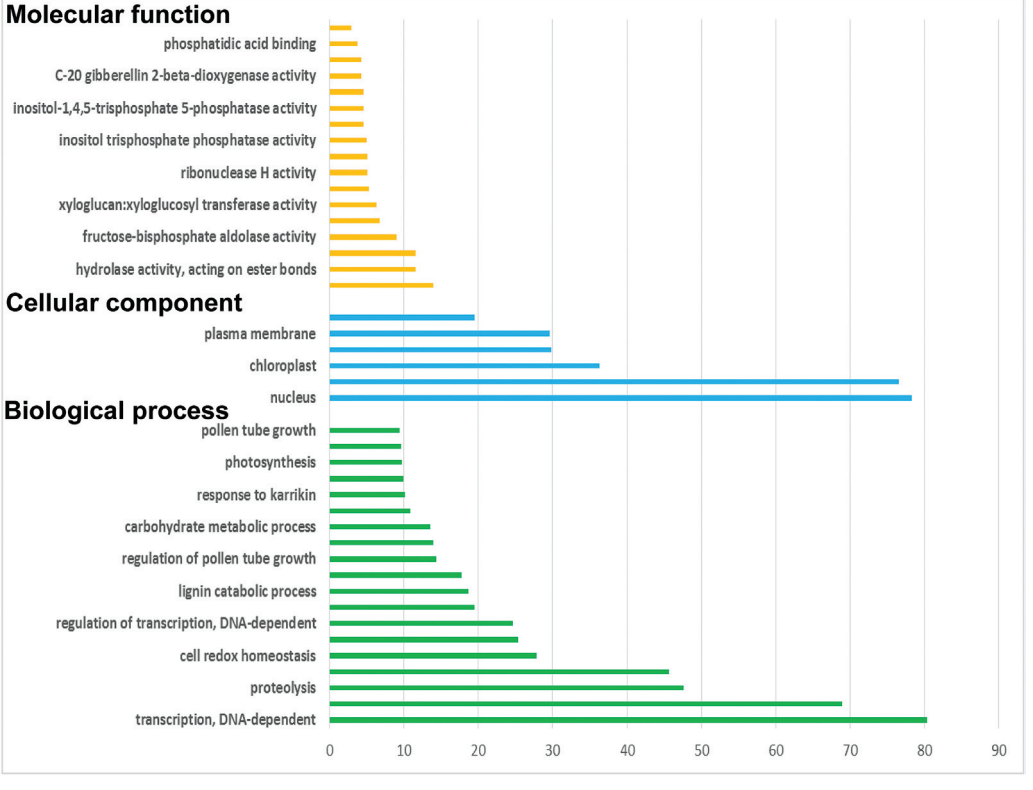

Fig. 2. GO terms for the top 1000 highly expressed transcripts in dwarf ylang ylang flowers. (This figure is available in colour at *JXB* online.)

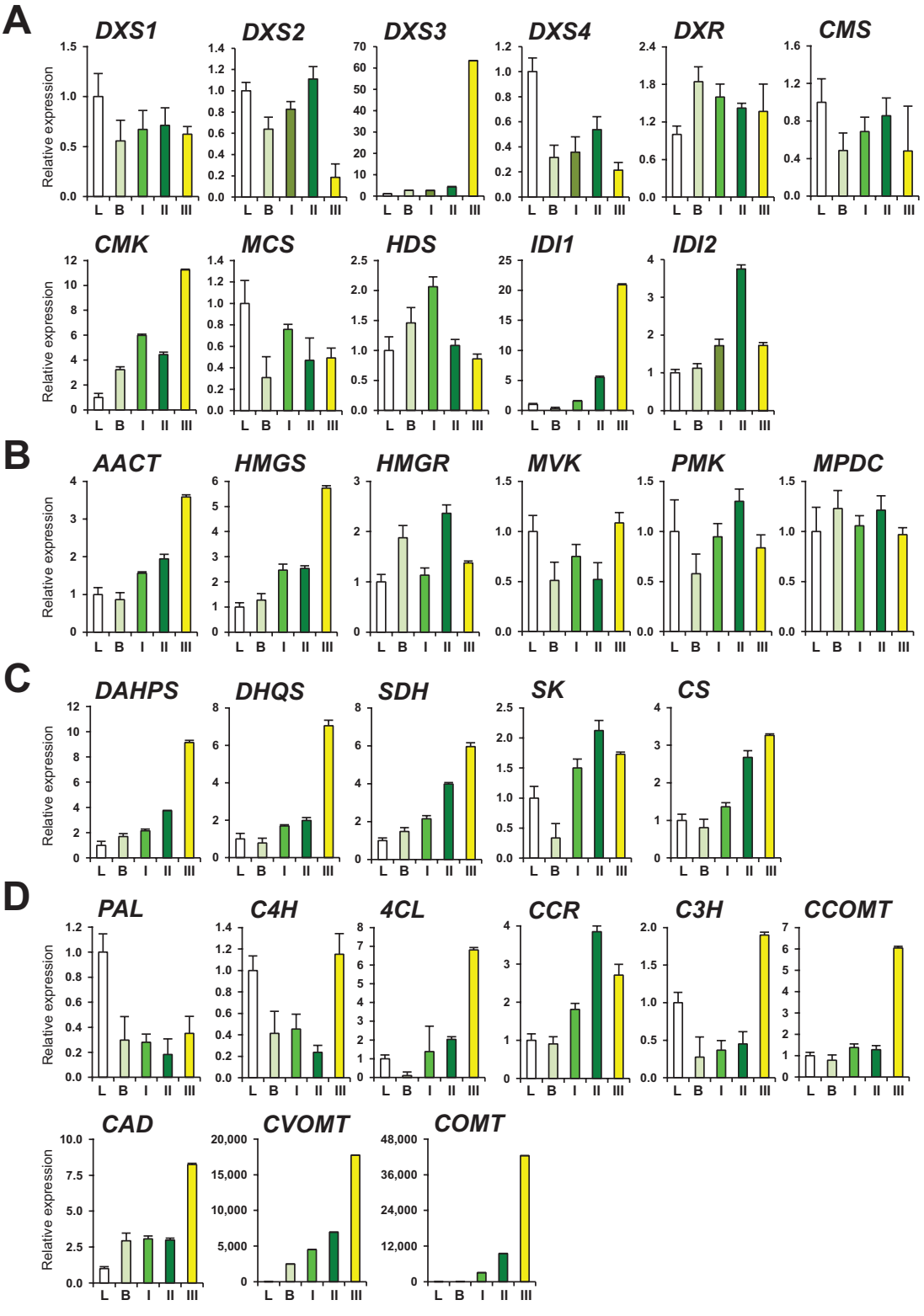

Fig. 3. qRT-PCR analyses of different biosynthetic pathway genes. Expression of genes involved in the MEP (A), MVA (B), shikimate (C), and phenyl propanoid (D) biosynthetic pathways were examined from leaves (L), buds (B), and three different stages of flower development: undeveloped small flowers (I), mature green flowers (II), and fully mature yellow flowers (III) by qRT- PCR. DXS, 1-deoxy-D-xylulose 5- phosphate synthase; DXR, 1-deoxy-D-xylulose 5-phosphate reductoisomerase; CMS, 2-C-methyl-D-erythritol 4-phosphate cytidylyltransferase; CMK, 4-(cytidine 5′-diphospho)-2-C-methyl-D-erythritol kinase; MCS, 2-C-methyl-D-erythritol 2,4-cyclodiphosphate synthase; HDS, 4- hydroxy-3-methylbut-2-en-1-yl diphosphate synthase; IDI, isopentenyl pyrophosphate isomerase; AACT, acetyl-CoA acetyltransferase; HMGS, hydroxymethylglutaryl-CoA synthase; HMGR, hydroxymethylglutaryl-CoA reductase; MVK, mevalonate kinase; PMK, phosphomevalonate kinase; MPDC, mevalonate diphosphate decarboxylase; DAHPS, 3-deoxy-D-arabino-heptulosonate-7-phosphate synthase; DHQS, 3-dehydroquinate synthase; SDH, shikimate dehydrogenase; SK, shikimate kinase; CS, chorismate synthase; PAL, phenylalanine ammonia lyase; C4H, cinnamate-4-hydroxylase; 4CL, 4-coumaroyl-CoA ligase; CCR, cinnamoyl-CoA reductase; C3H, *p*-coumarate-3-hydroxylase; CCOMT, caffeoyl-CoA 3-*O*-methyltransferase; CAD, cinnamyl alcohol dehydrogenase; CVOMT, chavicol *O*-methyltransferase; COMT, caffeic acid/5-hydroxyferulic acid *O*-methyltransferase. (This figure is available in colour at *JXB* online.)

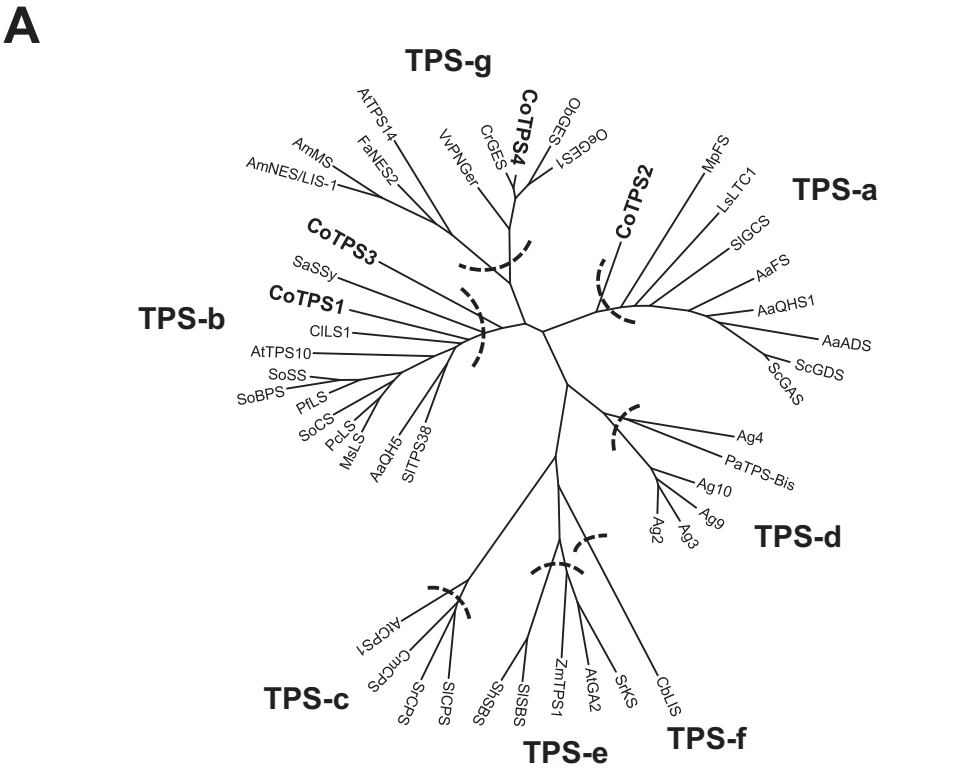

B

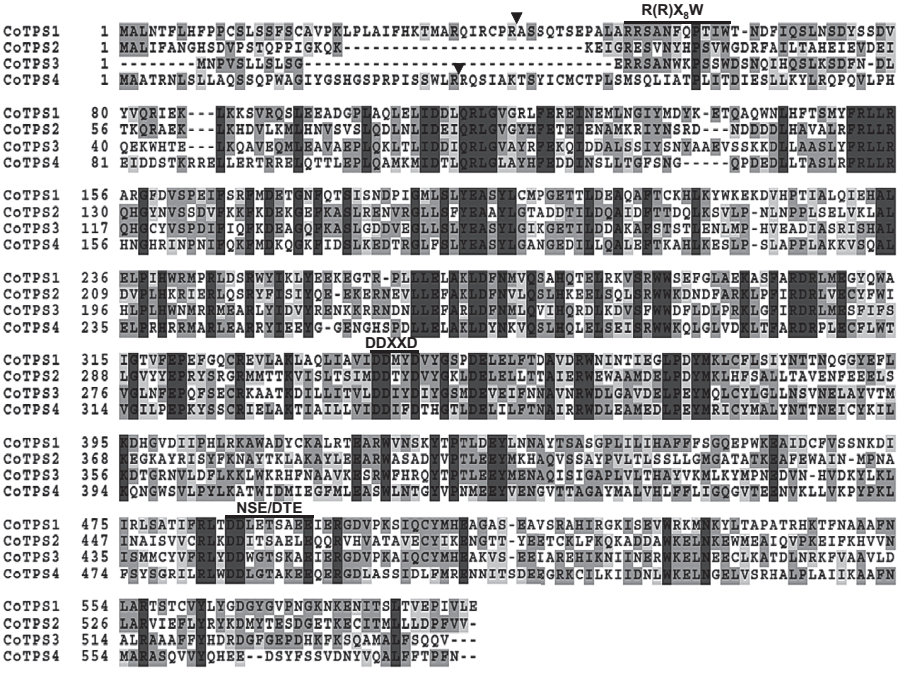

Fig. 4. Phylogenetic analysis and alignment of TPSs from dwarf ylang ylang. (A) A maximum likelihood tree was drawn using the MEGA 6 program from an alignment of full-length CoTPSs with other plant TPSs. The seven TPS subfamilies a–g are delimited by dashed lines, based on the taxonomic distribution of the TPS families (Chen *et al.*, 2011). AaADS, *Artemisia annua* (Aa) amorpha-4,11-diene synthase (NCBI Protein no. AFA34434); AaFS, β-farnesene synthase (Q9FXY7); AaQHS1, β-caryophyllene synthase (AAL79181); AaQH5, linalool synthase (AAF13356); Ag10, *Abies grandis* (Ag) 4S-limonene synthase (AAB70907); Ag2, myrcene synthase (AAB71084); Ag4, δ-selinene synthase (AAC05727); Ag3, pinene synthase (AAB71085); Ag9, terpinolene synthase (AAF61454); AmNES/LIS-1, *Antirrhium majus* (Am) nerolidol/linalool synthase1 (ABR24417); AmMS, myrcene synthase (AAO41727); AtCPS1, *Arabidopsis thaliana* (At) copalyl diphosphate synthase (NP_192187); AtGA2, kaurene synthase; AtTPS10 (AAC39443), myrcene/ocimene synthase (AAG09310); AtTPS14, linalool synthase (NP176361); CbLIS, *Clarkia breweri S*-linalool synthase (AAC49395); CILS1, *Citrus limon* limonene synthase 1 (AAM53944); CmCPS, *Cucurbits maxima* copalyl diphosphate synthase (AAD04292); CrGES, *Catharanthus roseus* geraniol synthase (AFD64744); FaNES2, *Fragaria×ananassa* nerolidol synthase (CAD57081); LsLTC1, *Lactuca sativus* germacrene A synthase (AAM11626); MpFS, *Mentha piperita* β-farnesene synthase (AAB95209); MsLS, *Mentha spicata* 4S-limonene synthase (AAC37366); ObGES, *Ocimum basilicum* geraniol synthase (AAR11765); OeGES1, *Olea europaea* geraniol synthase 1 (AFI47926); PaTPS-Bis, *Picea abies* α-bisabolene synthase (AAS47689);

had the conserved aspartate-rich motif (DDXXD) and NSE/DTE motifs that chelate divalent metal ions, typically Mg^{2+}, in the C-terminal domain (Fig. 4B). Both motifs are required for cyclization of the universal acyclic terpene precursors, such as GPP and FPP, to synthesize mono- and sesqui-terpene, respectively (Chen *et al.*, 2011). The arginine-tryptophan motif, R(R)X_8W, present at the N terminus of most mono-TPS and in some sesqui-TPS and di-TPS, was found in CoTPS1, CoTPS2, and CoTPS3 but not in CoTPS4 (Fig. 4B). One of the distinguishing structural features between mono- and sesqui-TPS is the presence of an N-terminal plastid transit peptide (Tp) sequence. Using the signal sequence analysis programs ChloroP (http://www.cbs.dtu.dk/services/ChloroP) and WoLF PSORT (http://www.genscript.com/psort/wolf_psort.html), a putative N-terminal plastid Tp sequence of 41 and 35 aa for CoTPS1 and CoTPS4, respectively, was predicted, indicating they are likely to be mono-TPSs. However, we could not find a putative plastid Tp sequence for CoTPS3, which was supposed to be a mono-TPS belonging to the TPS-b subfamily. CoTPS2 did not contain a plastid Tp sequence, which correlated well with the prediction of it being a sesqui-TPS.

The amino acid sequences of CoTPS1 and CoTPS2 had highest identity with the magnolia (*Magnolia grandiflora*) TPSs Mg17 (70% similarity, 54% identity) and Mg25 (72% similarity, 55% identity) for α-terpineol and β-cubebene, respectively (Supplementary Fig. S9A, B, available at *JXB* online) (Lee and Chappell, 2008). CoTPS3 showed 65% amino acid similarity and 47% identity with mountain pepper (*Litsea cubeba*) *trans*-ocimene synthase (Supplementary Fig. S9C) (Chang and Chu, 2011). CoTPS4 was most similar to geraniol synthase from Madagascar periwinkle (*Catharanthus roseus*) (92% similarity, 84% identity; Supplementary Fig. S9D) (Simkin *et al.*, 2013).

Subcellular localization and expression of the four CoTPSs

As well as phylogenetic analysis and bioinformatics-based attempts to classify TPSs, their subcellular localization is also important for function prediction. This was especially true for CoTPS3, since its function was unpredictable from the bioinformatics analyses based on amino acid sequences. To address this issue, we transiently expressed the full-length ORF of each CoTPS fused to a YFP reporter gene to produce a CoTPS–YFP fusion protein in *N. benthamiana* leaves using *Agrobacterium*-mediated infiltration. Figure 5 shows that CoTPS1–YFP and CoTPS4–YFP, which had the N-terminal plastid Tp sequence, were localized in chloroplasts as expected, whereas CoTPS2–YFP and CoTPS3–YFP were distributed throughout the cytosol. Based on the results of the subcellular localization experiments, it is likely that CoTPS1 and CoTPS4 are involved in monoterpene synthesis in plastids, whereas CoTPS2 and CoTPS3 might produce sesquiterpenes in the cytosol.

The transcript levels for the four *CoTPS* genes at different developmental stages of dwarf ylang ylang flowers were examined by qRT-PCR. The expression levels of all four transcripts were very low or below detection limits in leaf tissues but greatly elevated in flower tissues (Fig. 6). Transcripts for three *TPS* genes, *CoTPS1*, *CoTPS3*, and *CoTPS4*, were highest in mature green flowers (II), whereas *CoTPS2* was highly expressed at the floral bud stage (Fig. 6).

Functional characterization of CoTPSs

The subcellular localization of each CoTPS–YFP fusion protein provided us with preliminary evidence to elucidate the function of each TPS. The exact functional annotation of a new TPS requires activity characterization of the recombinant protein. To determine the enzymatic activity of CoTPSs *in vitro*, 6His-tagged CoTPS recombinant proteins purified from *E. coli* BL21(DE3) (Supplementary Fig. S10, available at *JXB* online) were used for *in vitro* assays. GPP (C10) or FPP (C15) was used as the common substrate for mono- and sesqui-TPS, respectively. Control assays using heat-inactivated recombinant 6His-tagged CoTPSs did not form any terpenes from GPP or FPP (Supplementary Fig. S11, available at *JXB* online). Figure 7A shows that CoTPS1, a member of the TPS-b family, synthesized four products corresponding to β-thujene, sabinene, β-pinene, and α-terpinene from GPP, but not from FPP, which were found in the essential oil profiles of dwarf ylang ylang flowers (#1, #4, #5 and #7, Fig. 1, Table 1). These results suggested that CoTPS1 is a multifunctional β-thujene/sabinene/β-pinene/α-terpinene synthase that is able to catalyse the synthesis of a mixture of monoterpenes, namely β-thujene, sabinene, β-pinene, and α-terpinene. This is not surprising, as several multiproduct mono-TPSs that produce similar compounds, such as α-thujene, sabinene, α/β-pinene, α/γ-terpinene, have been reported widely in other plant species (Lücker *et al.*, 2002; Chen *et al.*, 2003; Fäldt *et al.*, 2003; Shimada *et al.*, 2004; Fähnrich *et al.*, 2011).

PcLS, *Perilla citriodora* limonene synthase (AAG31435); PfLS, *Perilla frutescens* linalool synthase (AAL38029); SaSSy, *Santalum album* santalene/bergamotene synthase (ADO87000); ScGAS, *Solidago canadensis* (Sc) germacrene A synthase (CAC36896); ScGDS, germacrene D synthase (AAR31145); ShSBS, *Solanum habrochaites* santalene/bergamotene synthase (B8XA41); SlSBS, *Solanum lycopersicum* (Sl) santalene and bergamotene synthase (XP004244438); SlCPS, copalyl diphosphate synthase (BAA84918); SlGCS, germacrene C synthase (AAC39432); santalene/bergamotene synthase (BAA84918); Sl TPS38, Sl terpene synthase 38 (AEP82768); SoBPS, *Salvia officinalis* (So) bornyl diphosphate synthase (AAC26017); SoCS, 1,8-cineole synthase (AAC26016); SoSS, sabinene synthase (AAC26018); SrCPS, *Stevia rebaudiana* (Sr) copalyl pyrophosphate synthase (AAB87091); SrKS, kaurene synthase (AAD34294); VvPNGer, *Vitis vinifera* geraniol synthase (ADR74218); ZmTPS1, *Zea mays* terpene synthase 1 (AAO18435). (B) Comparison of deduced amino acid sequences of dwarf ylang ylang TPSs. The deduced amino acid sequences of *CoTPS* genes were aligned using CLUSTAL W. The Asp-rich domain DDXXD, the R(R)X_8W motif, and the NSE/DTE motif, which are highly conserved in plant TPSs and required for TPS activity, are indicated. Arrowheads denote the predicted cleavage sites of plastidial transit peptides. Completely conserved residues are shaded in dark grey, identical residues in grey, and similar residues in light grey. Dashes indicate gaps introduced to maximize sequence alignment.

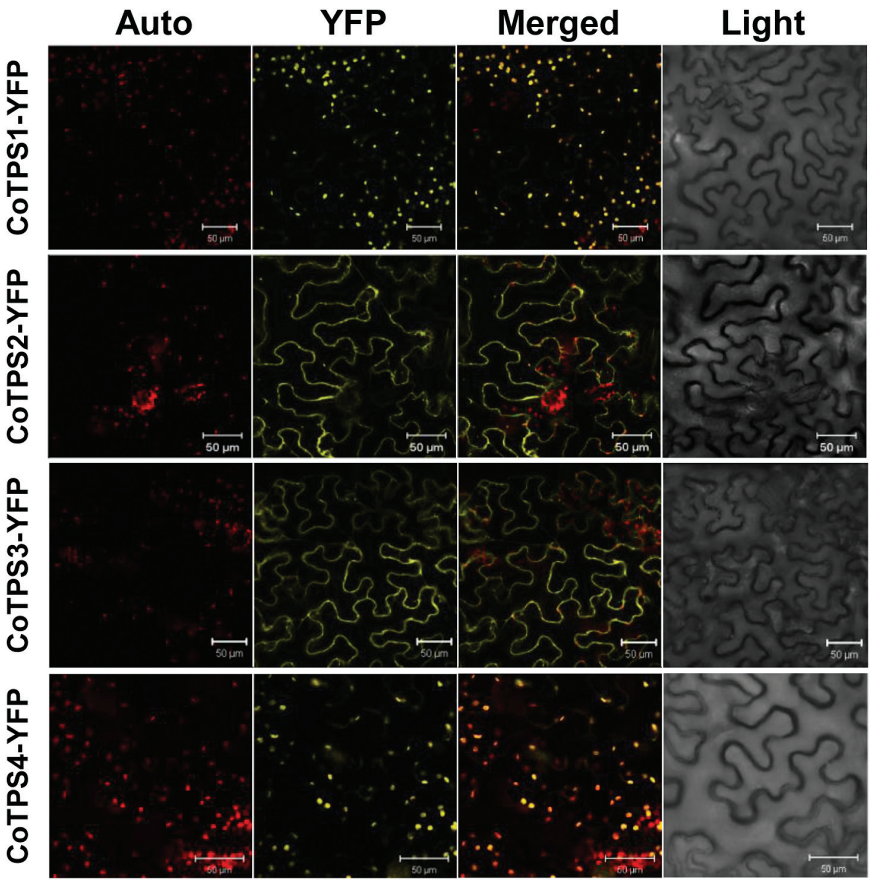

Fig. 5. Subcellular localization of CoTPSs. YFP-fused CoTPSs (CoTPS1–YFP, CoTPS2–YFP, CoTPS3–YFP, and CoTPS4–YFP) were transiently expressed in *N. benthamiana* leaves by *Agrobacterium*-mediated infiltration and visualized at 3 d post-infiltration using the YFP channel of a confocal microscope. Auto, chlorophyll autofluorescence; YFP, YFP channel image; Light, light microscopy image; Merged, merged image between Auto and YFP. Bars, 50 μm. (This figure is available in colour at *JXB* online.)

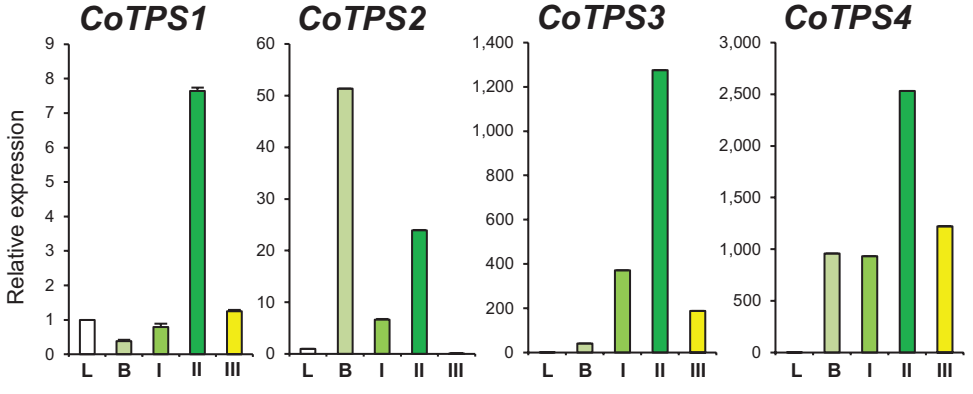

Fig. 6. Transcript levels of dwarf ylang ylang *TPS* genes *CoTPS1*, *CoTPS2*, *CoTPS3*, and *CoTPS4* during flower development. Total RNA was isolated from leaves (L), floral buds (B), and three different stages of flower development, undeveloped small flowers (I), mature green flowers (II) and fully mature yellow flowers (III), and used as template for qRT- PCR. Amplification of *Actin* mRNA was used as an internal control. (This figure is available in colour at *JXB* online.)

Similarly, recombinant CoTPS2 catalysed the synthesis of three compounds, β-ylangene, β-copaene, and β-cubebene, from FPP. CoTPS2 is a multifunctional β-ylangene/β-copaene/β-cubebene synthase capable of producing three sesquiterpenes, β-ylangene, β-copaene, and β-cubebene (Fig. 7B). Many sesqui-TPSs are also known to be multifunctional (Steele *et al.*, 1998; Lee and Chappell, 2008). However, TPSs that produce β-ylangene/β-copaene/β-cubebene have not yet been reported. Of these three sesquiterpene compounds, we could only detect β-ylangene and β-cubebene in the flowers of dwarf ylang ylang (#23 and #27, Fig. 1, Table 1).

CoTPS3 is a member of the TPS-b family with the unusual feature that it lacks a putative N-terminal Tp sequence. Our enzyme assays showed that CoTPS3 catalysed the formation of α-bergamotene from FPP (Fig. 7C), which is a major sesquiterpene produced in the flowers of ylang ylang (#30, Fig. 1, Table 1). CoTPS4, which belongs to TPS-g family, was capable of utilizing GPP to synthesize an acyclic

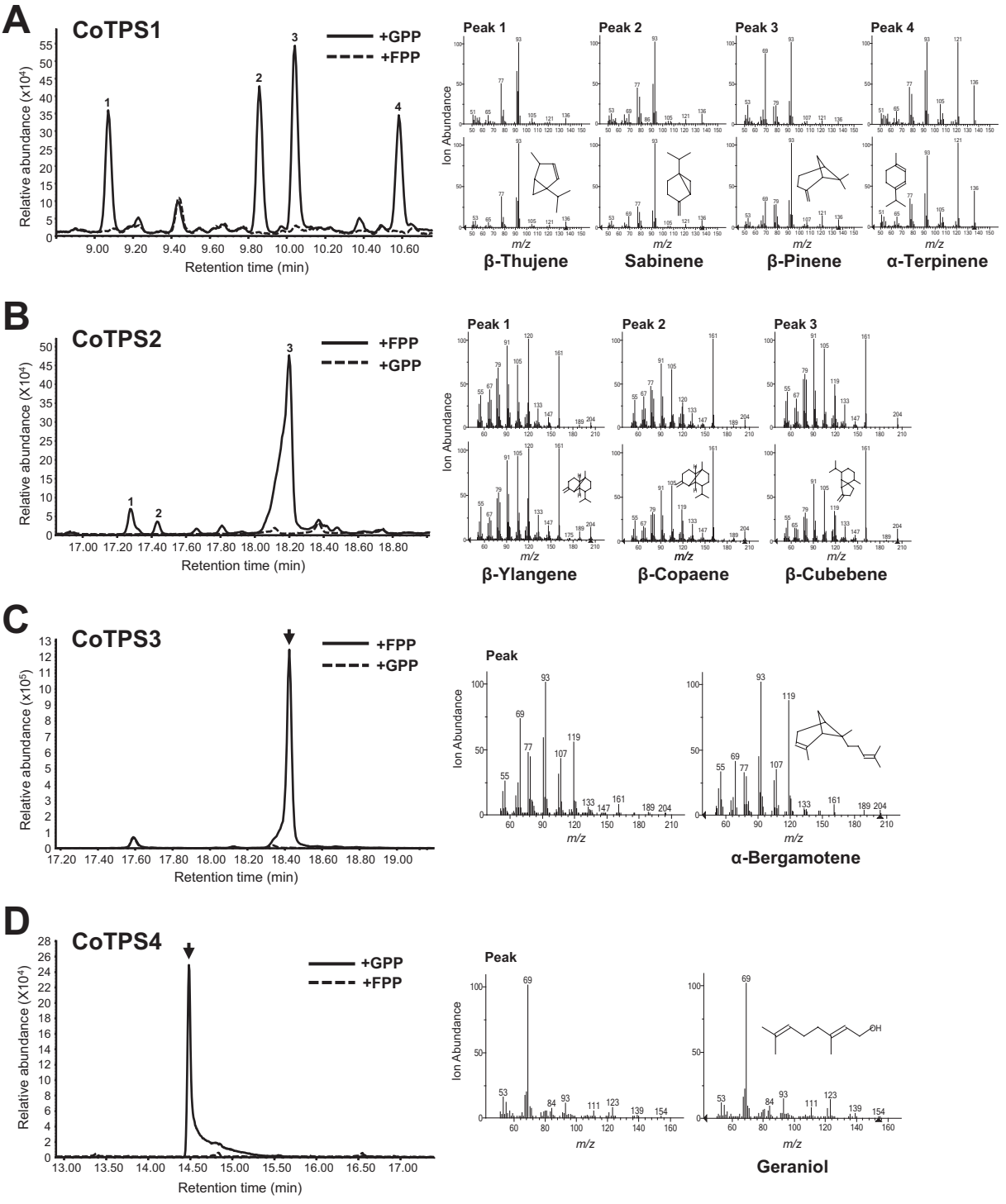

Fig. 7. *In vitro* enzymatic assays of recombinant CoTPSs. *In vitro* enzyme assays of recombinant 6His-tagged CoTPS1 (A), CoTPS2 (B), CoTPS3 (C), or CoTPS4 (D) protein using GPP or FPP as substrate. The reaction products were analysed by GC-MS. The peaks marked with numbers or an arrow in the GC traces were identified by the mass spectra reference library. Mass spectra for the peaks formed with FPP or GPP are shown on the right side of the figure with the references. *m/z*, Mass-to-charge ratio.

monoterpene, geraniol (Fig. 7D). This was confirmed by comparison of retention time and mass spectra with those of an authentic standard (Supplementary Fig. S11). This result was expected, as the protein showed the highest amino acid identity with geraniol synthases (84%) from Madagascar periwinkle (Supplementary Fig. S9D) (Simkin *et al.*, 2013). However, geraniol was not detected in our GC-MS analysis of ylang ylang flowers.

Functional characterization of CoTPS in vivo

We further investigated whether CoTPSs would produce the same terpene products *in vivo* using *Agrobacterium*-mediated transient gene expression in tobacco leaves. The YFP-fused CoTPS1, CoTPS2, CoTPS3, or CoTPS4 was expressed in *N. benthamiana* with or without co-expression of *Arabidopsis* HMGR. HMGR catalyses a rate-limiting step of the MVA

pathway and its overexpression is known to increases heterologous sesquiterpene production (Song *et al.*, 2012; Jin *et al.*, 2014). Analysis by GC-MS showed that the *in vivo* results were consistent with those obtained *in vitro*. CoTPS2–YFP clearly produced three compounds, β-ylangene, β-copaene, and β-cubebene, when it was co-expressed with AtHMGR (Fig. 8A), whereas Co-TPS3 produced α-bergamotene when co-expressed with AtHMGR (Fig. 8B). The expression of CoTPS2 or CoTPS3 alone without AtHMGR in *N. benthamiana* did not produce any terpenes, which may be due to limiting amounts of the substrate, FPP (Supplementary Fig. S12, available at *JXB* online). CoTPS1 and CoTPS4 characterized as mono-TPS *in vitro* failed to produce any new peaks *in planta*, suggesting that they might require the co-expression of additional genes, probably a rate-limiting step in the non-MVA pathway. Alternatively, compounds formed by these TPSs might be further metabolized endogenously by the plants.

Discussion

Dwarf ylang ylang essential oils are quantitatively dominated by sesquiterpene compounds

Plants use the vibrant colours and VOCs of flowers to attract pollinators. Our analysis on volatile essential oils of dwarf ylang ylang flowers (*C. odorata* var. *fruticosa*) showed that over 90% of the volatile essential oils is composed of sesquiterpenes, such as α-farnesene (31.50%), α-bergamotene (26.79%), germacrene D (13.26%), β-caryophyllene (11.57%), humulene (1.63%), farnesol (0.75%), *trans*-β-farnesene (0.77%), and β-ylangen (0.63%) (Fig. 1, Table 1). In addition, we also detected other groups of aromatic compounds such as benzyl benzoate, benzyl salicylate, and eugenol from the flowers of dwarf ylang ylang, but they constituted,3% (Table 1). This is very different from the composition of essential oils reported previously from ylang ylang flowers originating from Madagascar (Gaydou *et al.*, 1986). In our variety, we found a dominance of α-farnesene (31.50%) which was absent from Madagascar ylang ylang and α-bergamotene (26.79%) one of the main constituents of sandalwood oil (Jones *et al.*, 2011). The differences in the chemical composition of essential oils may be due to differences in genetic background, geographical location, growth conditions, and extraction methods (Benini *et al.*, 2012; Brokl *et al.*, 2013). Fragrant flowers from champak (*Michelia champaca* L.), indian cork (*Millingtonia hortensis* L.), and jasmine (*Jasminum sambac* L.) produce high amounts of four sesquiterpenes, β-caryophyllene, β-bergamotene, α-cubebene, and β-cubebene (Samakradhamrongthai *et al.*, 2009). β-Caryophyllene was the most abundant sesquiterpene in scented flowers of *Alstroemeria* cv. Sweet Laura,

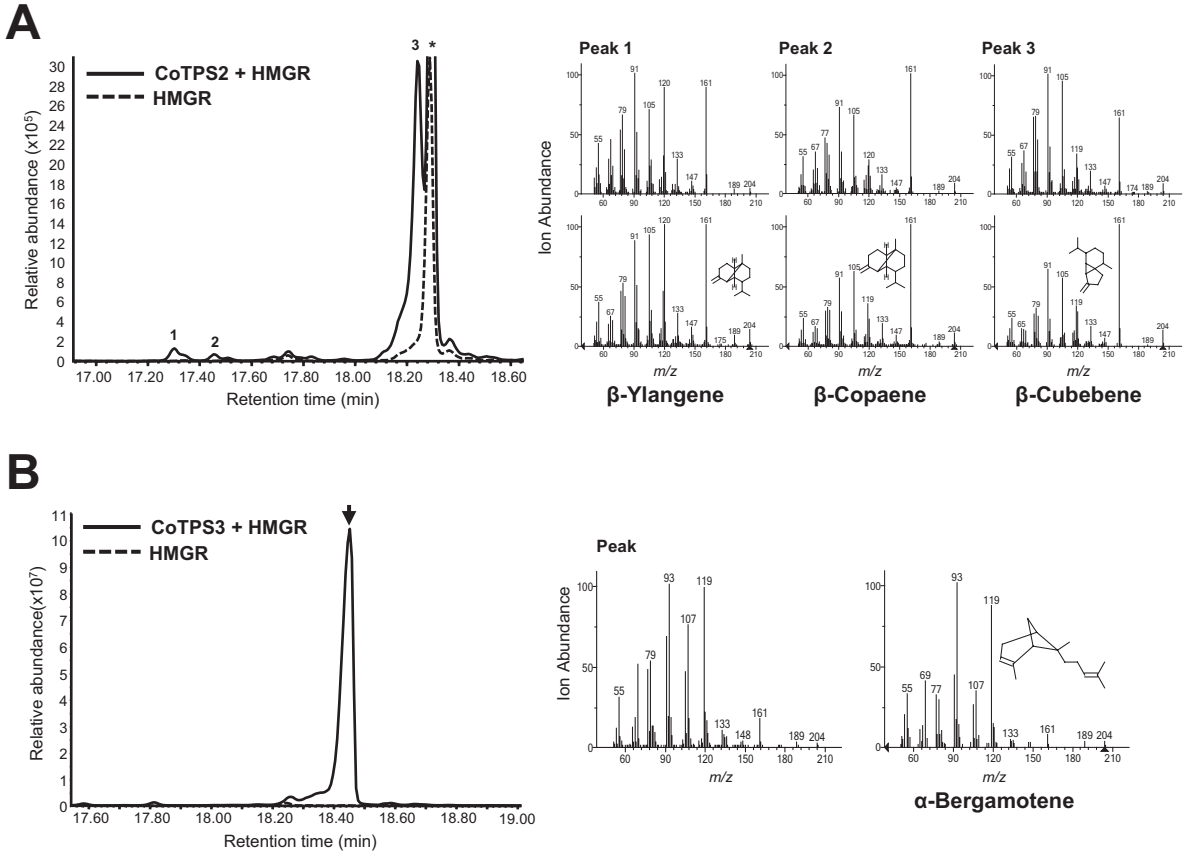

Fig. 8. *In vivo* characterization of CoTPS2 and CoTPS3. YFP-fused CoTPS2 (A) or CoTPS3 (B) with or without HMGR was transiently expressed in *N. benthamiana* leaves by *Agrobacterium*-mediated infiltration. The compounds were analysed at 3 d post-infiltration by GC-MS. Numbered peaks or an arrow in the GC traces were identified by the mass spectra reference library, and the mass spectra of compounds are shown on the right side. The expression of HMGR alone in each figure was used as a control. The asterisk indicates a non-specific peak derived from the expression of HMGR in *N. benthamiana* leaves. *m/z*, Mass-to-charge ratio.

which is one of only two scented commercial hybrids (Aros *et al.*, 2012). Therefore, these sesquiterpenes are likely to be important contributors to typical fragrances of these flowers. In addition to α-farnesene, we also detected high levels of β-caryophyllene and α-bergamotene in our ylang ylang variety.

Detection of TPS *genes from dwarf ylang ylang by RNA-seq*

Our RNA-seq approach provided a rich resource to identify and functionally characterize *TPS* genes from the flowers of dwarf ylang ylang. We found approximately 16 candidate *TPS* transcripts for various mono- and sesquiterpenes from the transcriptome data of dwarf ylang ylang flowers. However, many of the candidate *TPS* transcripts contained partial mRNA sequences from our RNA-seq data. Among the four *CoTPS* transcripts studied, the expression level of *CoTPS1* was the highest, followed by *CoTPS2* and *CoTPS3*, with *CoTPS4* being the lowest. However, the RNA-seq expression level of *CoTPS* transcripts did not correlate exactly with the abundance of terpenes produced by these TPSs when analysed by GC-MS. This might be due to post-translational modifications or may be a reflection of different enzyme activities.

Sequence characteristics of CoTPSs

According to our phylogenetic analysis, CoTPS1 and CoTPS3 were grouped in the TPS-b subfamily, which commonly represents angiosperm mono-TPSs. Generally, the TPS-b group contains two distinct structural domains, the plastid Tp domain and the R(R)X_8W motif for monoterpene cyclization located in N-terminal region of mature TPS (Bohlmann *et al.*, 1998). CoTPS1 appears to be a typical member of the TPS-b subfamily, and has both these mono-TPS characteristics. *In vitro* studies also showed that CoTPS1 catalysed the formation of a mixture of monoterpenes, β-thujene, sabinene, β-pinene and α-terpinene from GPP. In contrast to CoTPS1, CoTPS3 had a conserved R(R)X_8W motif but no Tp sequence for plastid targeting, which explained its cytosolic localization in transient expression assays (Fig. 5). Moreover, CoTPS3 used FPP to synthesize the sesquiterpene α-bergamotene *in vitro* and produced the same product *in vivo* (Figs 7C and 8B). Hence, it is a unique sesqui-TPS that not only contains the monoterpene characteristic R(R)X_8W but also belongs to the TPS-b subfamily associated with mono-TPSs. The protein encoded by *CoTPS3* had a low level of sequence identity of 45–47% to the α-terpineol synthase and *trans*-ocimene synthase from magnolia flower and mountain pepper, respectively, which are mono-TPSs most similar to CoTPS3 (Lee and Chappell, 2008; Chang and Chu, 2011). Similar sesqui-TPSs that reside in the TPS-b phylogenetic clade have been reported in tomato (*Solanum lycopersicum*) and sandalwood (*Santalum album*) (Falara *et al.*, 2011; Jones *et al.*, 2011). Conversely, the CoTPS4 contained the N-terminal 35 aa of a putative plastid Tp sequence but lacked the R(R)X_8W motif, a characteristic feature of TPS-b mono-TPSs. CoTPS4 was annotated as a plastid geraniol synthase by BlastX analysis, since it closely resembled the geraniol synthase from Madagascar periwinkle, with an amino acid sequence identity of 84% (Simkin *et al.*, 2013). As expected, this protein catalysed the synthesis of geraniol from GPP *in vitro*. Since the new TPS-g family lacking the R(R)X_8W motif was first defined from snapdragon *TPS* genes related to floral scent biosynthesis (Dudareva *et al.*, 2003), additional *TPS* genes belonging to the TPS-g family have subsequently been identified from *Arabidopsis*, rice, and kiwifruit. These TPSs produce acyclic terpenes, linalool and (*E*)-nerolidol (Yuan *et al.*, 2008; Chen *et al.*, 2011; Green *et al.*, 2012), which eventually became a prominent feature for members of the TPS-g group. As expected from a member of the TPS-g family, CoTPS4 produced an acyclic geraniol, and the protein sequence clustered closely with the grapevine geraniol synthases of the TPS-g subfamily (Martin *et al.*, 2010), indicating that these TPS functions are highly conserved among plants.

CoTPS2 is a multifunctional and novel sesqui-TPS

Many TPSs are known to synthesize several products simultaneously. Typical multiproduct mono-TPSs such as cineole synthases, terpinene synthases, terpinolene synthases, bornyl diphosphate synthases, carene synthases, and myrcene synthases additionally produce the same compounds such as sabinene, α/β-pinene (Lücker *et al.*, 2002; Chen *et al.*, 2003; Fäldt *et al.*, 2003; Shimada *et al.*, 2004; Fähnrich *et al.*, 2011). Most of the multiproduct TPSs are likely to synthesize one or two compounds dominantly as major products and others as minor components. Interestingly, CoTPS1 was capable of producing all four monoterpenes β-thujene, sabinene, β-pinene, and α-terpinene at similar levels, and was named β-thujene/sabinene/β-pinene/α-terpinene synthase in this study. Monoterpene thujene, usually referred to as α-thujene, has two double-bond isomers known as β-thujene and sabinene. As all thujene synthases identified catalyse the α form, CoTPS1 possessed the ability to cyclize GPP to β-thujene, found in dwarf ylang ylang flowers.

Some sesqui-TPSs belonging to the TPS-a subfamily from magnolia and kiwifruit preserve the N-terminal R(R)X_8W motif (Lee and Chappell, 2008; Nieuwenhuizen *et al.*, 2009). This was the case with CoTPS2 in this study. CoTPS2 was able to synthesize three kinds of sesquiterpenes, β-ylangene, β-copaene, and β-cubebene (Figs 7 and 8). Similar to CoTPS2, many sesqui-TPSs derived from different plant species have been documented to produce multiple products, which normally arise from enantiomers or common intermediates (Munck and Croteau, 1990; Steele *et al.*, 1998; Mercke *et al.*, 1999; Lee and Chappell, 2008).

Almost all the terpenes produced by the four CoTPSs are present in the ylang ylang essential oils composition as shown in Fig. 1 and Table 1, as well from other sources (Gaydou *et al.*, 1986; Brokl *et al.*, 2013). The two undetectable compounds, geraniol and β-copaene, may be produced in extremely small quantities and possibly could be detected by improved analytical technology such as two-dimensional GC-coupled time-of-flight MS. However, it remains to be

clarified whether these two compounds are indeed constituents of dwarf ylang ylang floral VOCs.

TPSs for α-bergamotene and geraniol have been reported in other plant species (Lu *et al.*, 2002; Iijima *et al.*, 2004; Landmann *et al.*, 2007). However, exclusive β-ylangene/β-copaene/β-cubebene synthases have not yet been reported. β-Cubebene synthase gene has been identified in *Magnolia grandiflora* (Lee and Chappell, 2008), as *Mg25*, sharing 55% amino acid sequence identity and 72% similarity to CoTPS2. β-Ylangene/β-cubebene or β-copaene/β-cubebene were found as minor peaks out of a total of 52 or 15 sesquiterpenes synthesized in *in vitro* assays in *Abies grandis* or *Medicago truncatula* (Steele *et al.*, 1998; Arimura *et al.*, 2008). Interestingly, a fungal (*Coprinus cinereus*) sesqui-TPS that synthesizes 10 different sesquiterpenes with δ-cadinene and β-copaene as the major products was capable of synthesizing β-ylangene, when the amino acid residues that presumably interact with a conserved Asp in the two metal-binding motifs were mutated (Lopez-Gallego *et al.*, 2010). β-Ylangene is a diastereomer of β-copaene; however, it was not produced by the wild-type sesqui-TPS (Lopez-Gallego *et al.*, 2010). In conclusion, CoTPS2 is a multifunctional and novel TPS producing three sesquiterpenes, β-ylangene, β-copaene, and β-cubebene, *in vitro* as well as *in vivo*. α-Copaene, the isomer of β-copaene, is a potent attractant for an agricultural pest, Mediterranean fruit flies, *Ceratitis capitata* (Nishida *et al.*, 2000). Future work should address the ecological role of these terpenes in environmental adaptation.

Supplementary data

Supplementary data are available at *JXB* online.

Supplementary Fig. S1. Compositional variation of dwarf ylang ylang essential oils during flower development.

Supplementary Fig. S2. Total ion chromatograms of essential oils from dwarf ylang ylang flowers.

Supplementary Fig. S3. Variation of four major terpenes during flower development.

Supplementary Fig. S4. Total ion chromatograms of essential oils from dwarf ylang ylang flowers sampled at day and night.

Supplementary Fig. S5. Quality of deep sequencing.

Supplementary Fig. S6. Alignment of deduced amino acid sequences of representative genes involved in biosynthetic pathways for VOCs.

Supplementary Fig. S7. Phylogenetic analysis of DXSs from dwarf ylang ylang.

Supplementary Fig. S8. Comparison of deduced amino acid sequences of four CoDXS small gene family.

Supplementary Fig. S9. Alignment of deduced amino acid sequences of CoTPSs and other plant TPSs.

Supplementary Fig. S10. SDS-PAGE gel showing purified recombinant 6His-tagged CoTPS1, CoTPS2, CoTPS3, and CoTPS4 proteins.

Supplementary Fig. S11. *In vitro* enzymatic assay of recombinant 6His-tagged CoTPS4s using GPP.

Supplementary Fig. S12. Transient expression of CoTPS2-YFP or YFP in *N. benthamiana.*

Supplementary Table S1. Oligonucleotide primers used in this study.

Acknowledgements

We thank the Rockefeller University sequencing facility and Dr Hui-Wen Wu for RNA-seq and the Temasek Life Sciences Laboratory central facilities for support with confocal microscopy. This research was funded by a grant from the Singapore National Research Foundation (Competitive Research Programme Award No. NRF-CRP8-2011-02) to SR and ICJ. JJ was partially supported by a Singapore Ministry of Education Tier-2 grant, MOE2009-T2-2–004.

References

Arimura G, Garms S, Maffei M, Bossi S, Schulze B, Leitner M, Mithöfer A, Boland W. 2008. Herbivore-induced terpenoid emission in *Medicago truncatula*: concerted action of jasmonate, ethylene and calcium signaling. *Planta* **227,** 453–464.

Aros D, Gonzalez V, Allemann RK, Müller CT, Rosati C, Rogers HJ. 2012. Volatile emissions of scented *Alstroemeria* genotypes are dominated by terpenes, and a myrcene synthase gene is highly expressed in scented *Alstroemeria* flowers. *Journal of Experimental Botany* **63,** 2739–2752.

Benini C, Danflous JP, Wathelet JP, du Jardin P, Fauconnier ML. 2010. Ylang-ylang [*Cananga odorata* (Lam.) Hook. f. & Thomson]: an unknown essential oil plant in an endangered sector. *Biotechnology, Agronomy, Society and Environment* **14,** 693–705.

Benini C, Mahy G, Bizoux JP, Wathelet JP, du Jardin P, Brostaux Y, Fauconnier ML. 2012. Comparative chemical and molecular variability of *Cananga odorata* (Lam.) Hook.f. & Thomson forma genuina (ylang-ylang) in the Western Indian Ocean Islands: implication for valorization. *Chemistry and Biodiversity* **9,** 1389–1402.

Bohlmann J, Meyer-Gauen G, Croteau R. 1998. Plant terpenoid synthases: molecular biology and phylogenetic analysis. *Proceedings of the National Academy of Sciences, USA* **95,** 4126–4133.

Brokl M, Fauconnier ML, Benini C, Lognay G, du Jardin P, Focant JF. 2013. Improvement of ylang-ylang essential oil characterization by GC×GC-TOFMS. *Molecules* **18,** 1783–1797.

Burdock GA, Carabin LG. 2008. Safety assessment of ylang-ylang oil as a food ingredient. *Food and Chemical Toxicology* **46,** 433–445.

Chang YT, Chu FH. 2011. Molecular cloning and characterization of monoterpene synthases from *Litsea cubeba*. *Tree Genetics and Genomes* **7,** 835–844.

Chen F, Tholl D, Bohlmann J, Pichersky E. 2011. The family of terpene synthases in plants: a mid-size family of genes for specialized metabolism that is highly diversified throughout the kingdom. *The Plant Journal* **66,** 212–229.

Chen F, Tholl D, D'Auria JC, Farooq A, Pichersky E, Gershenzon J. 2003. Biosynthesis and emission of terpenoid volatiles from Arabidopsis flowers. *The Plant Cell* **15,** 481–494.

Cordoba E, Porta H, Arroyo A, San Roman C, Medina L, Rodriguez-Concepcion M, Leon P. 2011. Functional characterization of the three genes encoding 1-deoxy-D-xylulose 5-phosphate synthase in maize. *Journal of Experimental Botany* **62,** 2023–2038.

Degenhardt J, Köllner TG, Gershenzon J. 2009. Monoterpene and sesquiterpene synthases and the origin of terpene skeletal diversity in plants. *Phytochemistry* **70,** 1621–1637.

Dudareva N, Cseke L, Blanc VM, Pichersky E. 1996. Evolution of floral scent in *Clarkia*: novel patterns of *S*-linalool synthase gene expression in the *C. breweri* flower. *The Plant Cell* **8,** 1137–1148.

Dudareva N, Klempien A, Muhlemann JK, Kaplan I. 2013. Biosynthesis, function and metabolic engineering of plant volatile organic compounds. *New Phytologist* **198,** 16–32.

Dudareva N, Martin D, Kish CM, Kolosova N, Gorenstein N, Faldt J, Miller B, Bohlmann J. 2003. (E)-β-Ocimene and myrcene synthase genes of floral scent biosynthesis in snapdragon: function and expression of three terpene synthase genes of a new terpene synthase subfamily. *The Plant Cell* **15,** 1227–1241.

Dudareva N, Murfitt LM, Mann CJ, Gorenstein N, Kolosova N, Kish CM, Bonham C, Wood K. 2000. Developmental regulation of methyl benzoate biosynthesis and emission in snapdragon flowers. *The Plant Cell* **12,** 949–961.

Fähnrich A, Krause K, Piechulla B. 2011. Product variability of the 'cineole cassette' monoterpene synthases of related *Nicotiana* species. *Molecular Plant* , **4,** 965–984.

Falara V, Akhtar TA, Nguyen TT, *et al*. 2011. The tomato terpene synthase gene family. *Plant Physiology* **157,** 770–789.

Fäldt J, Martin D, Miller B, Rawat S, Bohlmann J. 2003. Traumatic resin defense in Norway spruce (*Picea abies*): methyl jasmonate-induced terpene synthase gene expression, and cDNA cloning and functional characterization of (+)-3-carene synthase. *Plant Molecular Biology* **51,** 119–133.

Gaydou EM, Randriamiharisoa R, Bianchini JP. 1986. Composition of the essential oil of Ylang-Ylang (*Cananga odorata* Hook Fil. et Thomson forma genuina) from Madagascar. *Journal of Agricultural and Food Chemistry* **34,** 481–487.

Grabherr MG, Haas BJ, Yassour M, *et al*. 2011. Full-length transcriptome assembly from RNA-Seq data without a reference genome. *Nature Biotechnology* **29,** 644–652.

Green SA, Chen X, Nieuwenhuizen NJ, Matich AJ, Wang MY, Bunn BJ, Yauk YK, Atkinson RG. 2012. Identification, functional characterization, and regulation of the enzyme responsible for floral (*E*)-nerolidol biosynthesis in kiwifruit (*Actinidia chinensis*). *Journal of Experimental Botany* **63,** 1951–1967.

Harju AT, Pennanen SM, Liesivuori J. 2004. The efficacy of benzyl benzoate sprays in killing the storage mite *Tyrophagus putrescentiae* (Acari: Acaridae). *Annals of Agricultural and Environmental Medicine* **11,** 115–119.

Hoballah ME, Stuurman J, Turlings TC, Guerin PM, Connétable S, Kuhlemeier C. 2005. The composition and timing of flower odour emission by wild *Petunia axillaris* coincide with the antennal perception and nocturnal activity of the pollinator *Manduca sexta*. *Planta* **222,** 141–150.

Huber FK, Kaiser R, Sauter W, Schiestl FP. 2005. Floral scent emission and pollinator attraction in two species of *Gymnadenia* (Orchidaceae). *Oecologia* **142,** 564–575.

Iijima Y, Gang DR, Fridman E, Lewinsohn E, Pichersky E. 2004. Characterization of geraniol synthase from the peltate glands of sweet basil. *Plant Physiology* **134,** 370–379.

Jang IC, Yang JY, Seo HS, Chua NH. 2005. HFR1 is targeted by COP1 E3 ligase for post-translational proteolysis during phytochrome A signalling. *Genes and Development* **19,** 593–602.

Jin J, Panicker D, Wang Q, Kim MJ, Liu J, Yin J-L, Wong L, Jang IC, Chua NH, Sarojam R. 2014. Next generation sequencing unravels the biosynthetic ability of spearmint (*Mentha spicata*) peltate glandular trichomes through comparative transcriptomics. *BMC Plant Biology* **14,** 292.

Jones CG, Moniodis J, Zulak KG, Scaffidi A, Plummer JA, Ghisalberti EL, Barbour EL, Bohlmann J. 2011. Sandalwood fragrance biosynthesis involves sesquiterpene synthases of both the terpene synthase (TPS)-a and TPS-b subfamilies, including santalene synthases. *Journal of Biological Chemistry* **286,** 17445–17454.

Kessler A, Baldwin IT. 2001. Defensive function of herbivore-induced plant volatile emissions in nature. *Science* **291,** 2104–2105.

Knudsen JT, Eriksson R, Gershenzon J, Stahl B. 2006. Diversity and distribution of floral scent. *Botanical Review* **72,** 1–120.

Knudsen JT, Tollsten L, Bergström LG. 1993. Floral scents—a checklist of volatile compounds isolated by head-space techniques. *Phytochemistry* **33,** 253–280.

Landmann C, Fink B, Festner M, Dregus M, Engel KH, Schwab W. 2007. Cloning and functional characterization of three terpene synthases from lavender (*Lavandula angustifolia*). *Archives of Biochemistry and Biophysics* **465,** 417–429.

Lee S, Chappell J. 2008. Biochemical and genomic characterization of terpene synthases in *Magnolia grandiflora*. *Plant Physiology* . **147,** 1017–1033.

Lopez-Gallego F, Waerzyn GT, Schmidt-Dannert C. 2010. Selectivity of fungal seaquiterpene synthases: role of the active site's H-1α loop in catalysis. *Applied Environmental Microbiology* **76,** 7723–7733.

Lu S, Xu R, Jia JW, Pang JH, Matsuda SPT, Chen XY. 2002. Cloning and functional characterization of a β-pinene synthase from *Artemisia annua* that shows a circadian pattern of expression. *Plant Physiology* **130,** 1335–1348.

Lücker J, El Tamer MK, Schwab W, Verstappen FW, van der Plas LH, Bouwmeester HJ, Verhoeven HA. 2002. Monoterpene biosynthesis in lemon (*Citrus limon*). cDNA isolation and functional analysis of four monoterpene synthases. *European Journal of Biochemistry* **269,** 3160–3171.

Martin DM, Aubourg S, Schouwey MB, Daviet L, Schalk M, Toub O, Lund ST, Bohlmann, J. 2010. Functional annotation, genome organization and phylogeny of the grapevine (*Vitis vinifera*) terpene synthase gene family based on genome assembly, FLcDNA cloning, and enzyme assays. *BMC Plant Biology* **10,** 226.

Martin DM, Fäldt J, Bohlmann J. 2004. Functional characterization of nine Norway Spruce TPS genes and evolution of gymnosperm terpene synthases of the TPS-d subfamily. *Plant Physiology* **135,** 1908–1927.

McGarvey DJ, Croteau R. 1995. Terpenoid metabolism. *The Plant Cell* **7,** 1015–1026.

Mercke P, Crock J, Croteau R, Brodelius PE. 1999. Cloning, expression, and characterization of epi-cedrol synthase, a sesquiterpene cyclase from *Artemisia annua* L. *Archives of Biochemistry and Biophysics* **369,** 213–222.

Muhlemann JK, Klempien A, Dudareva N. 2014. Floral volatiles: from biosynthesis to function. *Plant, Cell and Environment* **37,** 1936–1949.

Munck SL, Croteau R. 1990. Purification and characterization of the sesquiterpene cyclase patchoulol synthase from *Pogostemon cablin*. *Archives of Biochemistry and Biophysics* **282,** 58–64.

Nieuwenhuizen NJ, Wang MY, Matich AJ, Green SA, Chen X, Yauk YK, Beuning LL, Nagegowda DA, Dudareva N, Atkinson RG. 2009. Two terpene synthases are responsible for the major sesquiterpenes emitted from the flowers of kiwifruit (*Actinidia deliciosa*). *Journal of Experimental Botany* **60,** 3203–3219.

Nishida R, Shelly TE, Whittier TS, Kaneshiro KY. 2000. α-Copaene, a potential rendezvous cue for the Mediterranean fruit fly, *Ceratitis capitata*? *Journal of Chemical Ecology* **26,** 87–100.

Orlova I, Marshall-Colón A, Schnepp J, *et al*. 2006. Reduction of benzenoid synthesis in petunia flowers reveals multiple pathways to benzoic acid and enhancement in auxin *transport. The Plant Cell* **18,** 3458–3475.

Phillips MA, Walter MH, Ralph SG, *et al*. 2007. Functional identification and differential expression of 1-deoxy-D-xylulose 5-phosphate synthase in induced terpenoid resin formation of Norway spruce (*Picea abies*). *Plant Molecular Biology* **65,** 243–257.

Quevillon E, Silventoinen V, Pillai S, Harte N, Mulder N, Apweiler R, Lopez R. 2005. InterProScan: protein domains identifier. *Nucleic Acids Research* **33,** W116–W120.

Samakradhamrongthai R, Utama-Ang M, Thakeow P. 2009. Identification of volatile compounds released from dry scented Thai flowers and their potential application in flower-mixed tea. *Asian Journal of Food and Agro-Industry* **2,** 525–534.

Shimada T, Endo T, Fujiia H, Hara M, Ueda T, Kita M, Omura M. 2004. Molecular cloning and functional characterization of four monoterpene synthase genes from *Citrus unshiu* Marc. *Plant Science* **166,** 49–58.

Simkin AJ, Miettinen K, Claudel P, *et al*. 2013. Characterization of the plastidial geraniol synthase from Madagascar periwinkle which initiates the monoterpenoid branch of the alkaloid pathway in internal phloem associated parenchyma. *Phytochemistry* **85,** 36–43.

Song AA, Abdullah JO, Abdullah MP, Shafee N, Othman R, Tan EF, Noor NM, Raha AR. 2012. Overexpressing 3-hydroxy-3-methylglutaryl coenzyme A reductase (HMGR) in the lactococcal mevalonate pathway for heterologous plant sesquiterpene production. *PLoS One* **7,** e52444.

Steele CL, Crock J, Bohlmann J, Croteau R. 1998. Sesquiterpene synthases from grand fir (*Abies grandis*): comparison of constitutive and wound-induced activities, and cDNA isolation, characterization, and bacterial expression of δ-selinene synthase and γ-humulene synthase. *Journal of Biological Chemistry* **273,** 2078–2089.

Tamura K, Peterson D, Peterson N, Stecher G, Nei M, Kumar S. 2011. MEGA5: molecular evolutionary genetics analysis using maximum likelihood, evolutionary distance, and maximum parsimony methods. *Molecular Biology and Evolution* **28,** 2731–2739.

Vogt T. 2010. Phenylpropanoid biosynthesis. *Molecular Plant* **3,** 2–20.

Voinnet O, Rivas S, Mestre P, Baulcombe D. 2003. An enhanced transient expression system in plants based on suppression of gene silencing by the p19 protein of tomato bushy stunt virus. *The Plant Journal* **9,** 949–956.

Walter M, Hans J, Strack D. 2002. Two distantly-related genes encoding 1-deoxy-D-xylulose 5-phosphate synthases: differential regulation in shoots and apocarotenoid-accumulating mycorrhizal roots. *The Plant Journal* **31,** 243–254.

Yuan JS, Köllner TG, Wiggins G, Grant J, Degenhardt J, Chen F. 2008. Molecular and genomic basis of volatile-mediated indirect defense against insects in rice. *The Plant Journal* **55,** 491–503.

Zhang X, Garreton V, Chua NH. 2005. The AIP2 E3 ligase acts as a novel negative regulator of ABA signaling by promoting ABI3 degradation. *Genes and Development* **19,** 1532–1543.